City and Built Environment

ORIGINAL ARTICLE Open Access

Estimation of regional anthropogenic heat from air conditioning systems and related devices in metropolitan commercial districts of Japan

Takahiro Ueno[1*], Eiko Kumakura[2] and Yasunobu Ashie[3]

*Correspondence:
ueno@aoni.waseda.com

[1] Waseda University, 3-4-1 Ookubo, Shinjuku-Ku, Tokyo 169-8555, Japan
[2] National Institute for Land and Infrastructure Management, 1 Tachihara, Tsukuba-City, Ibaraki 305-0802, Japan
[3] Building Research Institute, 1 Tachihara, Tsukuba-City, Ibaraki 305-0802, Japan

Abstract

With the expanding urban areas and increasing elderly population in Japan, anthropogenic heat poses substantial threat to human health. Air conditioning systems contribute to the anthropogenic heat from buildings. However, information regarding the heat characteristics of these systems is inadequate. In the present study, we developed a method for estimating anthropogenic heat from air conditioning, which accounts for most of the artificial heat from buildings during summer, to include artificial anthropogenic heat from surrounding buildings in the local heat risk assessment. The estimation results for commercial areas in Japan using the developed method showed that latent heat from air conditioning is substantially higher than sensible heat, and there was a difference in heat emissions between daytime and nighttime and between weekdays and holidays. A comparison of the calculation results of our method and those of previous studies showed no major differences in the orders of magnitude. With regard to the change in the amount of air-conditioning anthropogenic heat in the region, a directly proportional relationship was found between the outdoor temperature and the amount of air-conditioning anthropogenic heat. These results are useful for assessing the summer heat risk in urban areas and developing methods to mitigate the risks posed by urban heat.

Keywords: Artificial anthropogenic heat, Cooling demand, Air conditioning heat source, Cooling tower, Time series estimation

Introduction

The consumer sector, which consists of the residential and tertiary industrial sectors, accounts for a substantial portion of the final energy consumption in major countries, and its growth over time is significant. For example, the energy consumption density in Tokyo, the capital of Japan, is approximately 8.4 times higher than the national average (Agency for Natural Resources and Energy 2020), and there are concerns regarding the effects on atmospheric environment from the enormous energy consumption in the city. Energy consumption and anthropogenic heat are closely related, but their pathways and

characteristics are diverse. Therefore, understanding the actual situation, including the qualitative breakdown of local anthropogenic heat from buildings and traffic, to evaluate its effect on the atmospheric environment is important (Ashie et al. 2004).

Various studies have revealed the effects of heat damage on human health. Breitner et al. (2014) quantified the relationship between temperature and mortality in several German cities using time-series analysis combined with Poisson regression and distributed lag non-linear models and reported that very high air temperature increased cause-specific mortality. Basu (2009) examined the mortality evidence from elevated ambient temperatures in epidemiological studies and found a clear independent effect of temperature on mortality. Baccini et al. (2008) reported associations between maximum apparent temperature and mortality using daily data during the warm season in 15 European cities and found significant mortal effect of heat across Europe from June to August. Madaniyazi et al. (2016) evaluated the associations between temperature, heart rate, and blood pressure among 47,591 Chinese adults and reported that hot temperatures may have short-term effects on the heart rate and blood pressure. Ho et al. (2018) analyzed the short-term mortality risk using Poisson regression model to daily mortality data from 2007 to 2014 in Hong Kong and showed that a combined influence of haze, extreme weather/air quality, and the urban environment can result in extremely high mortality due to mental/behavioral disorders or diseases of the nervous system. Lin et al. (2022) evaluated the long-term health effects of anthropogenic heat exposure on blood pressure and hypertension and associated long-term anthropogenic heat exposure with elevated blood pressure and higher risk of hypertension. With the increasing population density in urban areas and global elderly population (United Nations 2022), these findings suggest that mitigation strategies for outdoor temperature rise and urban anthropogenic heat should be considered to curb health hazards. The number of health emergencies due to heat stroke is also increasing in Japan's aging population, and the heat stroke incidences have increased in years with many days of high temperatures or the occurrence of unusually high temperature days (Ministry of the Environment 2022). Therefore, reduction in anthropogenic heat is necessary for preventing heat stroke.

Furthermore, there have been several studies on anthropogenic heat from buildings. Ichinose et al. (1999) drew elaborate maps of anthropogenic heat in Tokyo using energy statistics data and a detailed digital geographic land use dataset, and discussed how reductions in energy consumption could mitigate the impacts on urban thermal environment. Yuan et al. (2022) proposed evidence-based strategies to improve residential building design in Singaporean residential neighborhoods to mitigate the negative effects of anthropogenic heat using computational fluid dynamics (CFD) models. Their numerical simulation indicated that the largest indoor temperature increment in naturally ventilated apartments caused by anthropogenic heat at the neighborhood scale was 4.2 °C. Li et al. (2019) reviewed the literature and observed that urban heat islands (UHI) can increase the cooling energy consumption in buildings. Considering the possibility that anthropogenic heat increases the UHI intensity (Kimura and Takahashi 1991), these findings suggest that anthropogenic heat has a spiraling effect that promotes energy consumption for building cooling in UHIs, which further intensifies UHI effect.

Various studies have developed methods for estimating the anthropogenic heat. Sailor (2011) suggested a roadmap for including anthropogenic heat and moisture in the urban

environment modeling based on a literature survey on the anthropogenic heating and opined that a combined inventory approach for industrial and transportation emissions and building energy modeling approach are ideal for including anthropogenic heat in atmospheric models. Jin et al. (2019) developed a new global gridded anthropogenic heat flux dataset with long-term time series using population density data and a top-down inventory-based approach. Their new global gridded dataset covers 1970–2050 and supports the simulation of climate change induced by anthropogenic heat. Chen and Hu (2017) estimated the high-resolution grid-scale anthropogenic heat flux over the Beijing–Tianjin–Hebei region in 2015 based on a developed parameterization scheme. The proposed parameterization scheme uses multisource remote sensing data to simplify the labor-intensive county-scale inventory approach. Bonifacio-Bautista et al. (2022) determined the main sources of anthropogenic heat flux based on vehicle classification, electricity consumption surveys, and population density in Mexico City and showed that vehicular traffic and electricity consumption contributed the most to anthropogenic heat flux. Hsieh et al. (2011) using a building energy program showed that heat rejection from air conditioners worsens the thermal environment below the urban canopy, thereby increasing building energy use. Ministry of Land, Infrastructure, Transport and Tourism, Ministry of the Environment (2004) also prepared inventory data on anthropogenic heat in Tokyo and showed the hourly anthropogenic heat intensity in August for offices, stores, hotels, and other buildings. Thus, various approaches, such as building energy modeling and energy consumption inventory, have been developed to estimate man-made heat emissions. In particular, the building energy modeling approach explicitly calculates the energy consumption of different building types and evaluates heat emissions based on energy consumption models. Using this method, the artificial heat exhaust from buildings has been accurately estimated (Heiple and Sailor 2008; Sailor 2011).

Because air conditioning systems contribute to the process of generating heat exhaust from buildings, several studies, as mentioned above, have analyzed the anthropogenic heat characteristics of these systems; however, the results are inadequate. To quantify the anthropogenic heat from building air conditioning in an area, understanding the regional configuration of air conditioning systems in the area, estimating the cooling demand and operation of air conditioning equipment based on the usage of each building, and accumulating the anthropogenic heat from each air conditioning system by considering outdoor air conditions are necessary. The current trends in global warming and expanding urban areas indicate a future in which heat risk reduction in urban areas will be earnestly considered.

Therefore, this study aims to incorporate artificial anthropogenic heat from surrounding buildings into the heat risk assessment of a specific area. We developed a method for estimating air-conditioning heat emissions from cooling, which accounts for the majority of artificial anthropogenic heat from buildings in urban commercial areas, and quantified the artificial anthropogenic heat from each building in the area subjected to calculation. The novelty of this study is the development of a methodology to calculate detailed sensible and latent heat quantities for each building in a commercial district through a building energy modeling method that integrates an estimation method of cooling demand considering building operating hours based on human flow data

analysis and an operation simulation method based on the installed configuration of air conditioning heat source equipment. The estimated latent and sensible heat data can be input into a CFD tool that evaluates the air and experienced temperatures of a city block to assess the heat risk to outdoor pedestrians (National institute for land and infrastructure management 2014; Ashie 2016).

Materials and methods

Study design

We developed a method for determining anthropogenic heat at five-minute intervals for each building using geographic information, human flow, and meteorological data. This method is based on that of a previous study (Ministry of Land, Infrastructure, Transport and Tourism, Ministry of the Environment 2004) along with updated configuration for heating, ventilation, and air-conditioning equipment efficiency, load characteristics, and reflected weather data for the target year 2019. Figure 1 shows the methodology used in this study. The estimation of anthropogenic heat is performed in three steps: cooling heat source equipment configuration, cooling demand estimation, and calculation of energy consumption and anthropogenic heat by cooling.

Nishi-Shinjuku area in Tokyo, which is included among the three major subcenters in Japan, was considered as the study area because it is a high-density commercial area with substantial air-conditioning anthropogenic heat emission. Table 1 summarizes the Nishi-Shinjuku 2-chome area, and Fig. 2 shows the gross floor area by building use. Figure 3 shows a map of the study area, which mainly consists of offices, stores, and hotels in the commercial districts. However, the percentage of residential buildings is small. Because 2019 was before the COVID-19 pandemic, telecommuting was not widespread and the number of people living in the homes during daytime was expected to be low. Therefore, the air conditioning anthropogenic heat generated from residential buildings in the target area was considered to be minimal compared to that from non-residential buildings; thus, this study deals only with air conditioning anthropogenic heat from non-residential buildings.

Composition of cooling heat source equipment

This section establishes the air conditioning heat source equipment configuration for each building based on the gross floor area and building use in the 2019 GIS data. Figure 4 shows the capacity intensity curves for the air-conditioning heat source equipment for each building use (Ueno et al. 2019). These curves show the cooling capacity of the heat source per unit gross floor area of the building. The air-conditioning equipment in non-residential buildings in this study were defined as absorption chillers (RHA), air-cooled electric chillers (AHP), and individually distributed packaged air conditioners (VRF). The composition of the cooling heat source equipment by building use was obtained from the data in a previous study (Ministry of Land, Infrastructure, Transport and Tourism, Ministry of the Environment 2004).

Cooling demand

Based on the basic start and end times set for each building use, the start and end times for non-residential buildings were set based on the number of commuters passing by

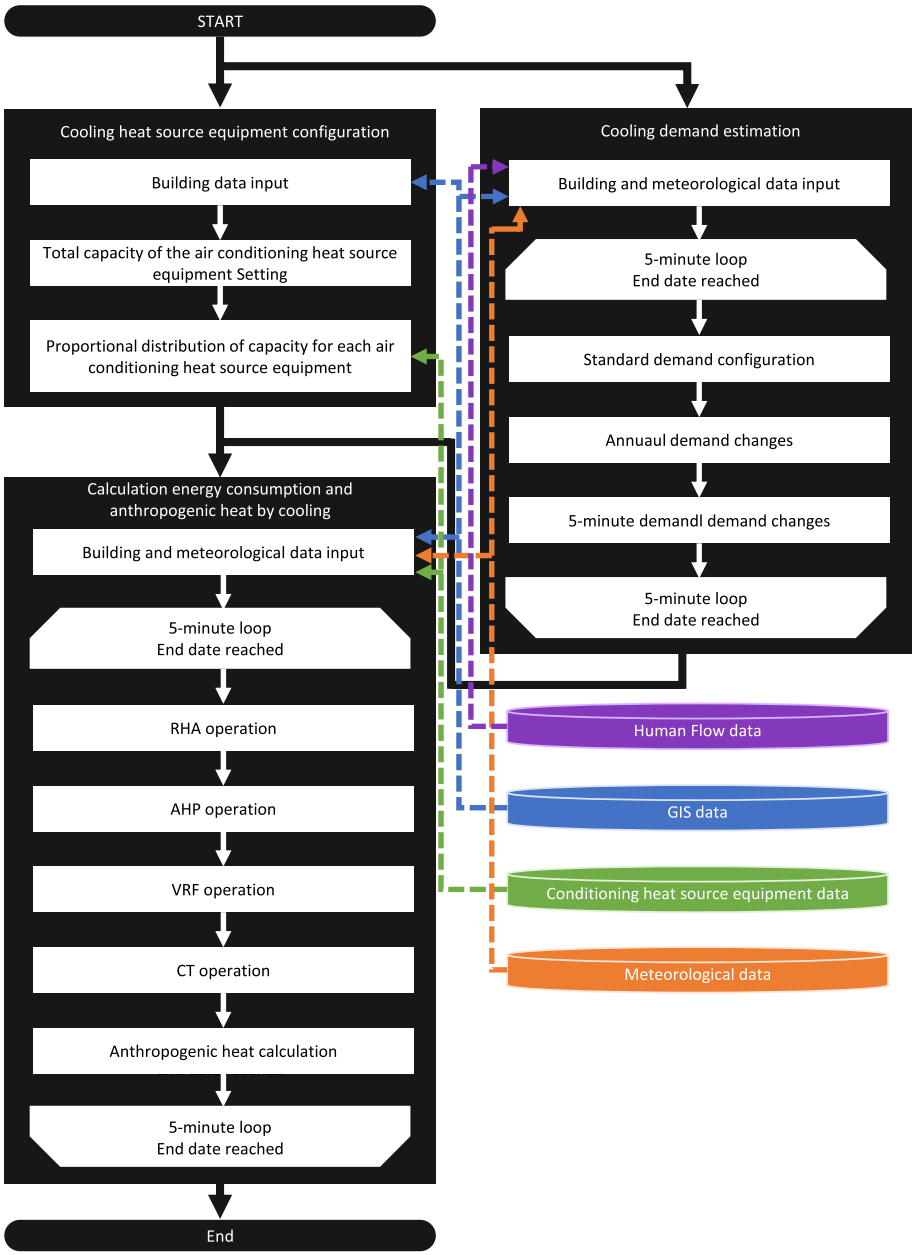

Fig. 1 Three-step determination of anthropogenic heat for buildings in Nishi-Shinjuku 2-chome area using geographic information, human flow, and meteorological data

Table 1 Summary of the Nishi-Shinjuku 2-chome area

Town and street	Nishi-Shinjuku 2-chome
Population	62 people
Number of Households	36 households
Area	338,255 m^2
Building gross floor area	1485,593 m^2
Floor–area ratio	439.19%

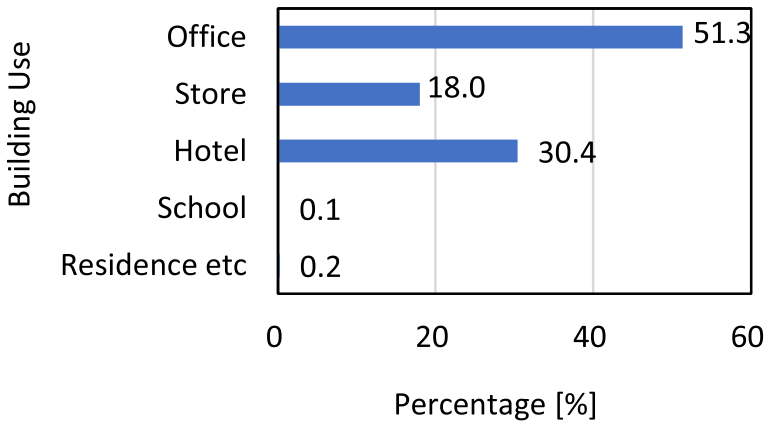

Fig. 2 Percentage total floor area by building use in Nishi-Shinjuku 2-chome

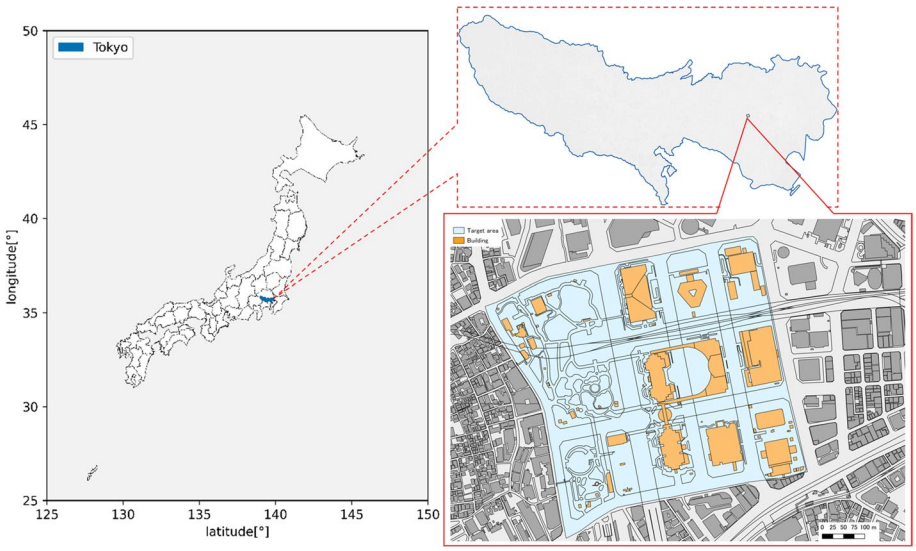

Fig. 3 Map showing the Nishi-Shinjuku area

each sidewalk at different times of the day using the current population data, linking each building to the nearest sidewalk using GIS software, and the number of people passing by each building daily during the target period.

We then estimated the five-minute interval heat source cooling demand for each building using a method developed in a previous study (Ueno et al. 2019), classified non-residential buildings in the city block into seven building types—hospital, hotel, office, store, school, restaurant, and others—and calculated the following equation for each building and time of the day to reproduce cooling demand fluctuations.

$$E_{Co(t)} = Ey_{Co} \cdot R_{Co(t)}/N_d \cdot A \cdot C(A) \cdot \mathrm{Ry} \cdot R(temp) \quad (1)$$

where $E_{Co\ (t)}$ is the cooling demand (MJ), Ey_{Co} is the annual cooling demand (MJ/m^2/year) by industry, $R_{Co\ (t)}$ is the ratio of annual cooling demand to time demand, N_d is the number of days of the week by month, A is the gross floor area (m^2) of the building, $C(A)$

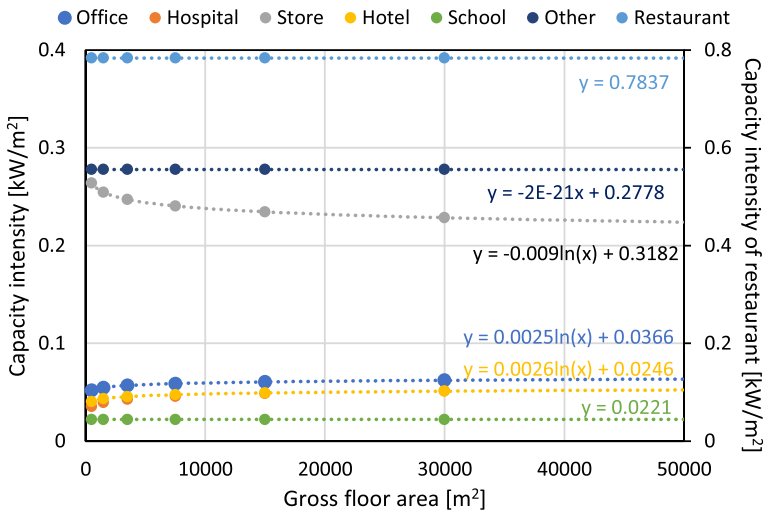

Fig. 4 Characteristic equations of the capacity curves of air-conditioning heat source equipment in various building use types

is the annual demand correction value by gross floor area, *Ry* is annual demand (MJ], and *R(temp)* is the cooling demand blip factor with outdoor temperature.

Energy consumption

Based on the air-conditioning heat source equipment model in the Building Energy Conservation Law ("Heisei 25nen jutaku•kenchikubutsu no shoenerugikijun kaisetsusho henshu iinkai" (2014); Fujii et al. 2009; Yanai et al. 2011), a model was constructed and used in this study to calculate the time-specific energy consumption of each building in the study area. The air-conditioning heat source equipment model first calculates the load factor of each air-conditioning heat source equipment based on cooling demand at five-minute intervals using Eq. 2. Because the rated capacity during actual operation increases or decreases depending on the cooling water temperature and outdoor air temperature, a quadratic function equation was set for each heat source model as the rated capacity characteristics from moment to moment in this calculation model. Second, energy consumption with time was calculated by inputting the load factor into the load characteristic formula set for each heat source model and multiplying the calculation result by the rated energy consumption (Eq. 3). Finally, Eq. 4 converts the electrical power to primary energy consumption and adds it with that of gas.

Similar to the rated capacity, the rated energy consumption quantity also increases or decreases depending on the cooling water temperature, water supply temperature, and outdoor air temperature. Figure 5(a) shows the capacity characteristic of heat source equipment depending on the outdoor temperature or cold-water temperature. Rated capacity, input, and refrigerant temperature characteristic equation has a range, and the value outside the range is constant at the range end, as shown by the dashed line in each figure. The rated capacity coefficient decreased as the temperature increased. Figure 5(b) shows the load characteristics. As the load factor decreased, the percentage energy consumption also decreased; however, the decreasing tendency differed depending on the heat source equipment. Figure 5(c) shows the input characteristics depending on the outdoor temperature

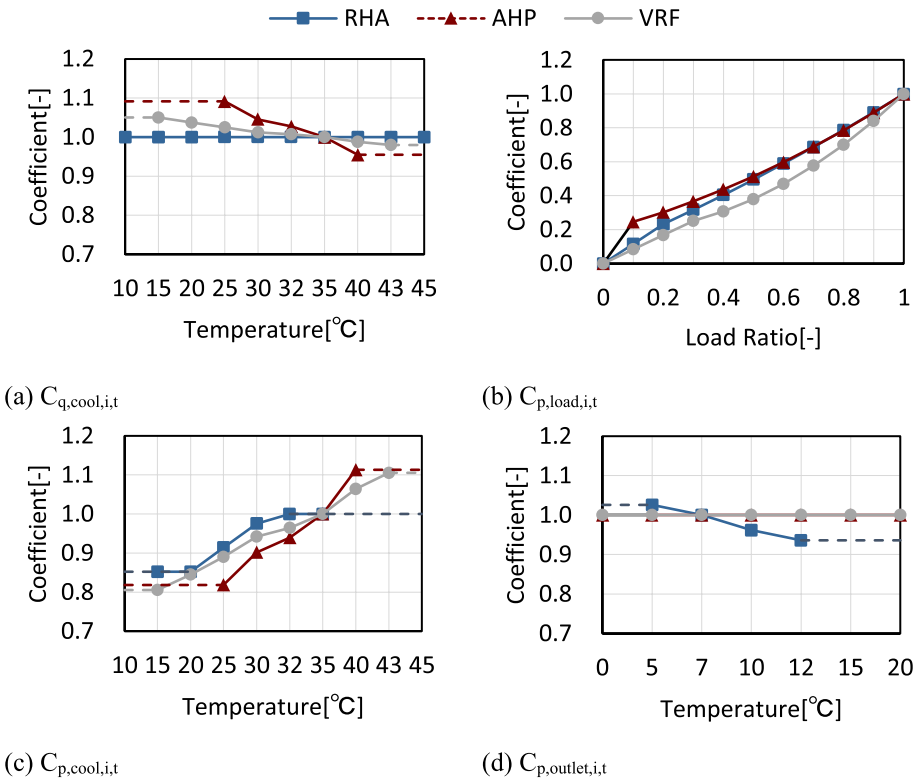

Fig. 5 **a** Rated capacity, **b** load, **c** input, and **d** refrigerant temperature characteristic trends of the air conditioning heat source equipment

or cold-water temperature. The rated input characteristics increased as the temperature increased. Figure 5(d) shows the refrigerant temperature characteristics of the heat-source equipment. The characteristics of the RHA increased by lowering the refrigerant temperature. However, the characteristics of the AHP and VRF were constant even when the refrigerant temperature changed. In the calculations, the refrigerant temperature was set to 7 °C according to the Building Energy Conservation Law. The system primary energy coefficient of performance (COP), which is the cooling demand of the entire building divided by the primary energy consumption of the entire air-conditioning heat source equipment, was calculated using Eq. 5 as an indicator of the heat source equipment efficiency.

$$L_{l,i,t} = \frac{Q_{i,t}}{q_{i,rated} \times C_{q,correct} \times C_{q,cool,i,t}} \tag{2}$$

$$E_{ele,i,t} \text{ or } E_{gas,i,t} = \frac{Q_{i,t} \times C_{p,correct}}{L_{e,i,rated} \times C_{p,load,i,t} \times C_{p,cool,i,t} \times C_{p,outlet,i,t}} \tag{3}$$

$$E_{prim,t} = C_{prim} \times \sum_i E_{ele,i,t} + \sum_i E_{gas,i,t} \tag{4}$$

$$COP_t = \frac{\sum_i Q_{i,t}}{E_{prim,t}} \tag{5}$$

where $L_{l,i,t}$ is the load ratio of heat source equipment i at time t, $Q_{i,t}$ is the cooling demand at time t (MJ), $q_{i,rated}$ is the rated cooling capacity of heat source equipment i (MJ), $C_{q,correct}$ is the correction coefficient in capacity of heat source equipment (=0.95), $C_{q,cool,i,t}$ is the capacity characteristic of heat source equipment i depending on outdoor temperature/cold water temperature at time t, $E_{ele,i,t}$ is the electricity consumption of heat source equipment i at time t (MJ), $E_{gas,i,t}$ is the gas consumption of heat source equipment i at time t (MJ), $C_{p,correct}$ is the correction coefficient in energy consumption of heat source equipment (=1.2), $L_{e,i,rated}$ is the rated cooling efficiency of heat source equipment i (AHP=3.7, RHA=1.08, VRF=2.67), $C_{p,load,i,t}$ is the load characteristic of heat source equipment i at time t, $C_{p,cool,i,t}$ is the input characteristic of heat source equipment i depending on outdoor temperature/cold water temperature at time t, $C_{p,outlet,i,t}$ is the refrigerant temperature characteristic of heat source equipment i at time t, $E_{prim,t}$ is the primary energy consumption at time t (MJ), and C_{prim} is the coefficient of primary energy conversion (=2.71) [-], COP_t: system primary energy COP at time t [-].

Anthropogenic heat

The amount of anthropogenic heat transferred to the atmosphere by air conditioning was calculated from the air-conditioning energy consumption of each building in terms of sensible heat and latent heat. Figure 6 shows the heat transport flow of the air-conditioning heat source. In the calculations, exhaust heat from the AHP and VRF were calculated as sensible heat, as it is derived from the power input and cooling demand (Eq. 6). For the RHA, the amount of heat from the exhaust gas was estimated from the combustion efficiency of the boiler and divided into sensible heat and latent heat (Eqs. 7 and 8).

The heat transferred from the RHA to the cooling tower was calculated as sensible heat and latent heat using a cooling tower model based on a previous study (Ashie et al. 1999). The cooling towers were all open-type counter-current cooling towers, and the inlet/outlet water temperatures of the cooling towers were calculated based on the circulating water quantity, air flow rate, and atmospheric conditions, corresponding to changes in the cooling load. The quantity of circulating water was set for each building according to the capacity of the air-conditioning heat source equipment, and the airflow

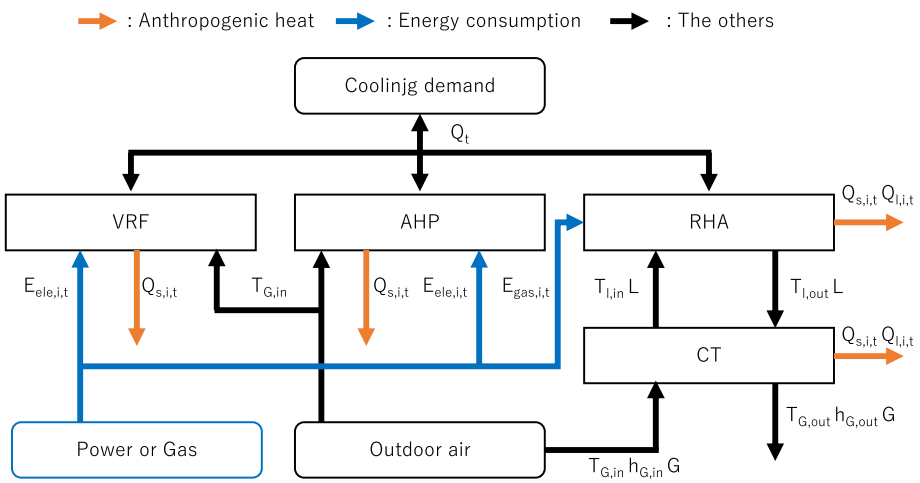

Fig. 6 Heat transport flow of the air conditioning heat source

rate of the cooling tower was also set for each building based on the amount of circulating water and the water–air ratio. The cooling tower characteristics for each building were set using the results of calculations based on Chebyshev's formula according to the Japanese Industrial Standards (Japanese Standards Association 2008). To quantify heat loss from the cooling tower, the temperature difference between the cooling water inlet and outlet and specific enthalpy of the outlet air were determined using Eq. 9. Furthermore, the operating line was drawn on the T·h diagram and the U/N value was calculated using Eq. 10. Subsequently, the combination of inlet/outlet temperatures of the cooling water that achieves the design value was obtained by iterative calculations based on the U/N value. The breakdown of the sensible and latent heat was obtained from Eqs. 11 and 12, respectively.

$$Q_{s,i,t} = Q_{i,t} + E_{ele,i,t} \tag{6}$$

$$Q_{s,i,t} = \delta \times (1-\zeta) \times E_{gas,i,t} \tag{7}$$

$$Q_{l,i,t} = (1-\delta) \times (1-\zeta) \times E_{gas,i,t} \tag{8}$$

$$\left(Q_{i,t} + \zeta \times E_{gas,i,t}\right) = G\left(h_{G,out,t} - h_{G,in,t}\right) = C_l L(T_{l,in,t} - T_{l,out,t}) \tag{9}$$

$$U/N = \int_{T_{l,out,t}}^{T_{l,in,t}} \frac{C_l dT}{h_s - h_l} \tag{10}$$

$$Q_{s,i,t} = G\left(C_{G,out,t} T_{G,out,t} - C_{G,in,t} T_{G,in,t}\right) \tag{11}$$

$$Q_{l,i,t} = \left(Q_{i,t} + \zeta \times E_{gas,i,t}\right) - Q_{s,i,t} \tag{12}$$

where $Q_{s,i,t}$ is the load ratio of heat source equipment i at time t [-], $Q_{i,t}$ is the cooling demand at time t [MJ], $E_{ele,i,t}$ is the electricity consumption of heat source equipment i at time t [MJ], $Q_{l,i,t}$ is the load ratio of heat source equipment i at time t [-], ζ is the cooling tower load ratio (=0.83) [-], δ is the percentage of sensible heat in combustion exhaust gas (=0.54) [-], $E_{gas,i,t}$ is the gas consumption of heat source equipment i at time t [MJ], G is the cooling tower airflow volume[kg/h], $h_{G,out,t}$ is the specific enthalpy of cooling tower outlet air at time t [kJ/kg(DA)], $h_{G,in,t}$ is the specific enthalpy of cooling tower inlet air at time t [kJ/kg(DA)], C_l is the specific heat of water (=4.217) [kJ/kg·K], L is the cooling tower water volume [kg/h], $T_{l,in,t}$ is the temperature of cooling tower inlet water at time t [℃], $T_{l,out,t}$ is the temperature of cooling tower outlet water at time t [℃], U/N is the number of transfer units [-], h_s is the specific enthalpy of operating line [kJ/kg(DA)], h_l is the saturated specific enthalpy [kJ/kg(DA)], $C_{G,out,t}$ is the specific heat of moist air at cooling tower outlet at time t [kJ/kg·K], $T_{G,out,t}$ is the temperature of cooling tower outlet air at time t [℃], $C_{G,in,t}$ is the specific heat of moist air at cooling tower inlet at time t [kJ/kg·K], and $T_{G,in,t}$ is the temperature of cooling tower inlet air at time t [℃].

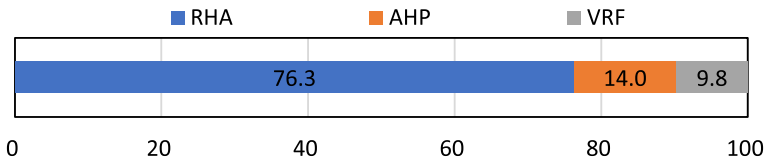

Fig. 7 Composition of cooling heat source equipment in Nishi-Shinjuku 2-chome area

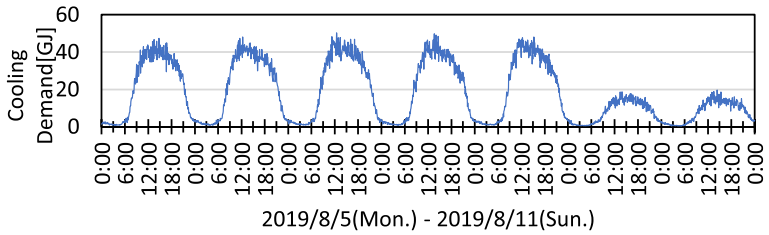

Fig. 8 Five-minute interval cooling demand during a representative week

Results

Composition of cooling heat source equipment

This section describes the calculation results of each step in the estimation of anthropogenic heat based on human flow data. By setting the air conditioning heat source equipment configuration for each building, the capacity of central heat source equipment, such as RHA and AHP, was confirmed to be approximately 90% of the total capacity of the area in Nishi-Shinjuku 2-chome area (Fig. 7). The total heat-source cooling capacity for the entire region was 133 MW (=479 GJ/h).

Cooling demand

The results of setting the start and end times of each building in this area based on human flow data indicated that there were some non-residential buildings in each area whose start and end times were approximately one–two hours ahead or behind the basic time. Figure 8 shows the results of the cooling demand estimation. By estimating the total daily district cooling demand in these areas, we confirmed that there were substantial differences between weekdays and holidays and between daytime and nighttime.

Primary energy consumption

Figure 9 shows the results of primary energy consumption. By estimating the total daily district cooling demand in these areas, we confirmed that there were substantial differences between weekdays and holidays and between daytime and nighttime. The average primary energy consumption was 5.7 TJ/day. The primary energy COP was 0.79 for the total calculation period.

Anthropogenic heat

Figure 10 shows the temporal variations in the sensible heat and latent heat. During daytime in summer, 79 GJ/h of sensible heat was generated. The total daily sensible heat on

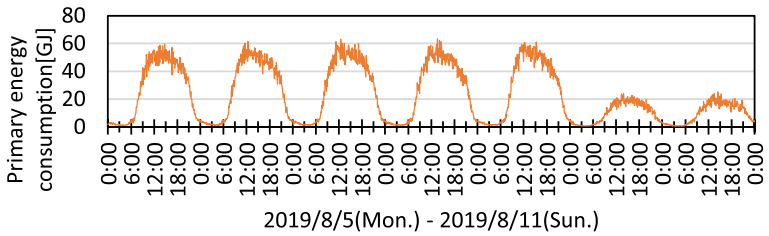

Fig. 9 Five-minute interval energy consumption during a representative week

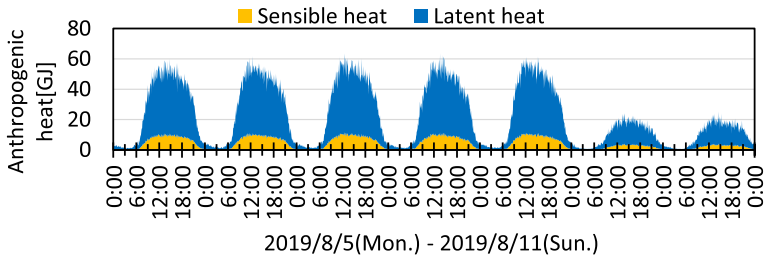

Fig. 10 Anthropogenic heat in five-minute intervals during a representative week

weekdays was 11 TJ/day. The latent heat generated by the air-conditioning heat source equipment and related equipment was 355 GJ/h during the daytime, accounting for approximately 82% of the total heat during the day.

Discussion

Summary of findings

We developed a method for calculating the air-conditioning anthropogenic heat in buildings and estimated it for commercial areas. Sensible and latent heat in August were calculated for a commercial area in Japan by setting up air-conditioning heat source equipment in each building. The results showed the following:

1) RHAs accounted for most of the heat source capacity in the target area.
2) The total time-specific cooling demand and energy consumption in the region differed substantially between daytime and nighttime and between weekdays and holidays. The primary energy COP of the system for the calculation period was 0.79.
3) District exhaust heat also exhibited similar time-series differences in cooling demand and energy consumption. During weekdays, 5 TJ/day of air-conditioning anthropogenic heat was released into the atmosphere.
4) The ratio of sensible to latent heat was approximately 1:4, with latent heat accounting for most of the air-conditioning anthropogenic heat during the day.

Cooling characteristics and energy conservation measures in the study area

Cooling demand to Anthropogenic heat showed large differences between the data on weekdays and weekends, and between daytime and nighttime. These differences were due to the building type, majority of which were office buildings, in the commercial districts. Therefore, the cooling demand, cooling energy consumption, and cooling

anthropogenic heat during night and holidays, which are after-hours for office buildings, were lower than those during the working hours.

As a large proportion of the consumer sector uses thermal comfort in commercial and residential buildings, improvement of the overall efficiency of air-conditioning systems in buildings is of positive significance in reducing the total energy consumption of society (Chua et al. 2013; Yang et al. 2014). Energy-saving options for air conditioning in the target area include the introduction of thermal energy storage systems, such as heat storage tanks, and more efficient air-conditioning equipment. Thermal energy storage systems offer advantages such as increased overall efficiency and reliability, improved economics, and lower operating costs (Navarro et al. 2016). In this area, a thermal storage system can improve the operating efficiency of air conditioning by using heat stored at night or early in the morning, when outdoor air temperatures are low, for daytime use. District heating and cooling systems are also effective options for this area. They are considered more efficient than individual air-conditioning systems and energy-saving solutions for space heating and cooling in high-demand density areas (European Union 2010, 2012). The peak cooling demand density in this area, the total demand during peak cooling hours divided by area, was 15.5 GJ/ha-h, which meets or exceeds 8 GJ/ha-h and is adequate to establish a heat supply business (Japan District Heating and Cooling Association 2013). The introduction of these technologies is expected to improve the energy efficiency in this area.

Comparison of the method with existing methods for anthropogenic heat estimation

To validate the accuracy of the model, we compared the calculated values of this calculation method with those estimated using the existing estimation methods (Ministry of Land, Infrastructure, Transport and Tourism, Ministry of the Environment 2004). The calculated values are the results of five-minute interval calculations for each building in the Nishi-Shinjuku 2-chome area from August 1 to 31, which were combined into hourly values for the total area and averaged into monthly values for each time. In contrast, estimated value from the previous study is the value obtained by multiplying the August time-specific air conditioning heat emission intensity by building use and total floor area shown in the previous study with the data for each building in the Nishi-Shinjuku 2-chome area and adding them with the area total. Figure 11 shows the comparison of the anthropogenic heat calculated using the present method and previous method. The comparison showed no major difference in the order during daytime. Improvements in the performance of air-conditioning heat source equipment are the reason for the smaller value in the present method compared to that of previous method during the daytime; further, because overtime hours have been extended, the value from the present method is larger than that from the previous method during the nighttime.

Primary energy consumption and system primary energy COP

Figure 12 shows the hourly system COP. The system COP shows time-series changes for all days; however, the pattern of change differs with days. The monthly average system COP increased during the morning and decreased during the day. On the highest temperature day of the month, the system COP appeared high during the nighttime because the heat source system operates at high efficiency, but the value during the daytime

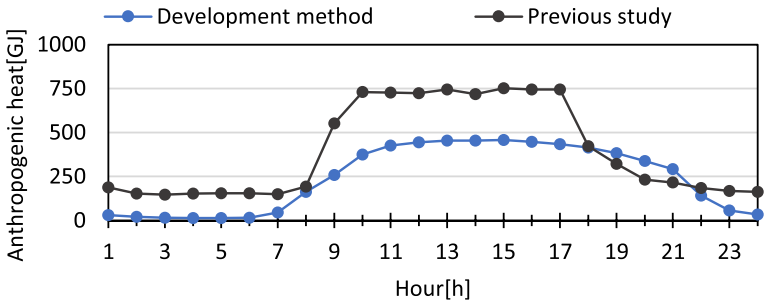

Fig. 11 Comparison of the anthropogenic heat estimation using the present developed method and that of the previous study

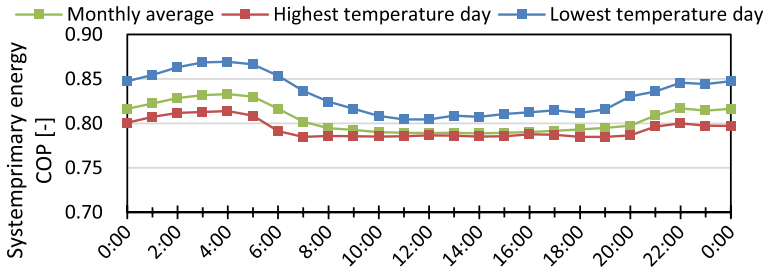

Fig. 12 Time-series system COP on the highest and lowest temperature days

declined owing to the adverse conditions of high temperatures. On the lowest temperature day of the month, the COP is high due to the lower temperatures increasing the heat source equipment efficiency.

Breakdown of building use with respect to anthropogenic heat

To indicate the breakdown of building use in anthropogenic heat, we averaged the five-minute interval calculation values for each building in the Nishi-Shinjuku 2-chome area from August 1 to 31 into the monthly average five-minute interval value and added for each building use. Figure 13 shows temporal variations in the building use. During the daytime, offices discharged the highest amount of heat, approximately 122 GJ/h of waste heat, while commercial buildings generated the largest amount of anthropogenic heat among building uses from 21:25 to 22:15; after 22:20, hotels dominated the heat discharge. From midnight to 06:00, anthropogenic heat was generated almost exclusively from the hotels, accounting for 3% of the daily value. Thus, the building use that generates the most exhaust heat differs according to the time of the day.

Temperature Effects

Figure 14 shows the relationship between the outdoor air temperature and heat dissipation. The overall trend is that as the outdoor air temperature increased, the air-conditioning anthropogenic heat increased. The anthropogenic heat during building operating hours (10:00 to 22:00) can be roughly divided into two groups: daytime and weekday, each of which linearly increased with outdoor air temperature. The anthropogenic heat during non-operating hours had a greater dispersion than that during operating hours, but it also tended to be proportional to the outdoor air temperature.

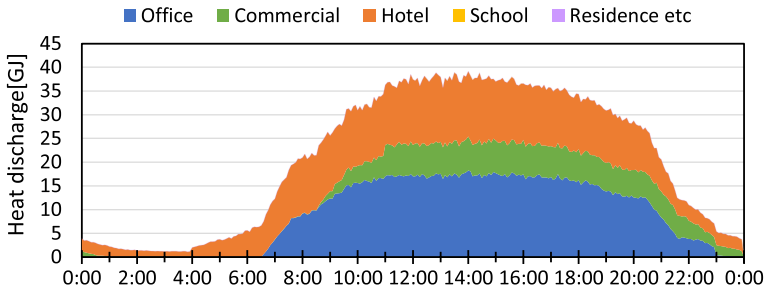

Fig. 13 Breakdown of building use in average monthly five-minute interval anthropogenic heat

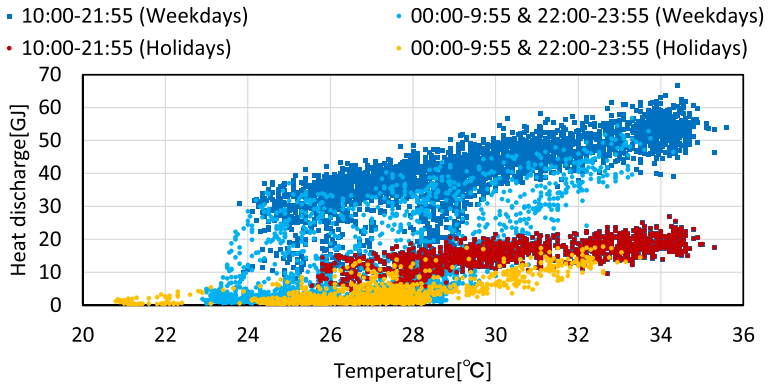

Fig. 14 Relationship between outdoor air temperature and anthropogenic heat

The phenomenon of an increase in air-conditioning anthropogenic heat due to rising summer temperatures is an important issue to consider when studying measures to reduce UHIs. Therefore, although there are various other possible influencing factors, such as the thermal capacity of each building and indoor heat generation conditions, studying the relationship between the amount of air-conditioning anthropogenic heat in a city block and the outdoor temperature is necessary to reduce the heat risk for pedestrians during the summer.

Conclusions

We developed a method for estimating anthropogenic heat from air conditioning, which accounts for most of the artificial heat from buildings during summer, to include artificial anthropogenic heat from surrounding buildings for the local heat risk assessment. The estimation results for commercial areas in Japan using the developed method showed that latent heat from air conditioning was several times higher than sensible heat in the study area and there was a difference in the heat generated between daytime and nighttime and between weekdays and holidays. A comparison of the calculation results of our method and those of previous studies showed no major differences in the orders of magnitude. Regarding the change in the amount of air-conditioning anthropogenic heat in the region, a direct proportional relationship was found between the outdoor temperature and amount of air-conditioning anthropogenic heat. These results are useful for assessing the summer heat risk in urban areas. In the future, we intend to assess

anthropogenic heat due to road traffic. Based on the aforementioned results, we plan to develop a pattern of summer anthropogenic heat from traffic and incorporate it into a CFD-based thermal environment assessment tool to evaluate thermal risk considering artificial anthropogenic heat and to study measures to reduce exposure to anthropogenic heat, such as securing urban airways and building layouts and application of covering materials as heat countermeasures.

Acknowledgements
This research was performed by the Environment Research and Technology De-velopment Fund (2-2106) of the Environmental Restoration and Conservation Agen-cy Provided by the Ministry of Environment of Japan.

Concise title
Air-conditioning anthropogenic heat estimation.

Authors' contributions
All authors contributed to the study conception and design. Material preparation, data collection and analysis were performed by Takahiro Ueno. The first draft of the manuscript was written by Takahiro Ueno and all authors commented on previous versions of the manuscript. All authors read and approved the final manuscript.

Funding
This research was funded by the Environment Research and Technology Development Fund (2–2106) of the Environmental Restoration and Conservation Agency Provided by the Ministry of Environment of Japan.

Availability of data and materials
Not applicable.

Declarations

Competing interests
The authors have no competing interests to declare that are relevant to the content of this article.

Received: 8 September 2022 Accepted: 22 April 2023
Published online: 23 June 2023

References

Agency for Natural Resources and Energy (2020) General Energy Statistics. https://www.enecho.meti.go.jp/statistics/total_energy/results.html. Accessed 15 Dec 2022

Ashie Y (2016) Simulation software for evaluating thermal environment measures in cities with simple operation. 4th International Conference on Countermeasures to Urban Heat Island (UHI 2016), Singapore.

Ashie Y, Li H, Yoon S (2004) Analysis of exhaustion characteristics of anthropogenic exhaustion heat considering the differences of sensible and latent heat in Tokyo 23 wards. Trans Soc Heat Air-conditioning Sanit Eng Jpn 29:121–130. https://doi.org/10.18948/shase.29.92_121

Ashie Y, Tanaka M, Yamamoto T (1999) Anthropogenic heat characteristics of air conditioning systems of office buildings. Trans Soc Heat Air-conditioning Sanit Eng Jpn 24:89–97. https://doi.org/10.18948/shase.24.75_89

Baccini M, Biggeri A, Accetta G, Kosatsky T, Katsouyanni K, Analitis A et al (2008) Heat effects on mortality in 15 European cities. Epidemiology 19:711–719. http://www.jstor.org/stable/25662618. Accessed 15 Dec 2022

Basu R (2009) High ambient temperature and mortality: a review of epidemiologic studies from 2001 to 2008. Environ Health 8:40. https://doi.org/10.1186/1476-069x-8-40

Bonifacio-Bautista M, Ballinas M, Jazcilevich A, Barradas VL (2022) Estimation of anthropogenic heat release in Mexico City. Urban Clim 43:101158. https://doi.org/10.1016/j.uclim.2022.101158

Breitner S, Wolf K, Devlin RB, Diaz-Sanchez D, Peters A, Schneider A (2014) Short-term effects of air temperature on mortality and effect modification by air pollution in three cities of Bavaria, Germany: A time-series analysis. Sci Total Environ 485–486:49–61. https://doi.org/10.1016/j.scitotenv.2014.03.048

Chen S, Hu D (2017) Parameterizing anthropogenic heat flux with an energy-consumption inventory and multi-source remote sensing data. Remote Sens 9:1165. https://doi.org/10.3390/rs9111165

Chua KJ, Chou SK, Yang WM, Yan J (2013) Achieving better energy-efficient air conditioning – a review of technologies and strategies. Appl Energy 104:87–104. https://doi.org/10.1016/j.apenergy.2012.10.037

European Union (2010) Directive 2010/31/EU of the European Parliament and of the Council of 19 May 2010 on the energy performance of buildings (recast). Official Journal of the European Union. https://eur-lex.europa.eu/LexUriServ/LexUriServ.do?uri=OJ:L:2010:153:0013:0035:EN:PDF. Accessed 07 Dec 2022

European Union (2012) Directive 2012/27/EU of the European Parliament and of the Council of 25 October 2012 on energy efficiency. Official Journal of the European Union. https://eur-lex.europa.eu/LexUriServ/LexUriServ.do?uri=OJ:L:2012:315:0001:0056:en:PDF. Accessed 07 Dec 2022

Fujii T, Murakami S, Ishino H, Yanai T (2009) Development of an integrated energy simulation tool for buildings and MEP systems, the BEST (Part51): Characteristics of heat source appliances and packaged air conditioners. Technical

Papers of Annual Meeting of the Society of Heating, Air-conditioning and Sanitary Engineers of Japan 2009.2:687–690.https://doi.org/10.18948/shasetaikai.2009.2.0_687
Heiple S, Sailor DJ (2008) Using building energy simulation and geospatial modeling techniques to determine high resolution building sector energy consumption profiles. Energy Build 40:1426–1436. https://doi.org/10.1016/j.enbuild.2008.01.005
"Heisei 25nen jutaku kenchikubutsu no shoenerugikijun kaisetsusho henshu iinkai" (2014) "Heisei 25nen shoeneru-gikijun ni junkyoshita santei handan no hoho oyobi kaisetsu I hijutakukenchikubutsu (dai2han)". "kabushiki kaisha rengo insatsu senta", Tokyo, pp 149–261.
Ho HC, Wong MS, Yang L, Shi W, Yang J, Bilal M, Chan TC (2018) Spatiotemporal influence of temperature, air quality, and urban environment on cause-specific mortality during hazy days. Environ Int 112:10–22. https://doi.org/10.1016/j.envint.2017.12.001
Hsieh C, Aramaki T (2011) Hanaki K (2011) Managing heat rejected from air conditioning systems to save energy and improve the microclimates of residential buildings. Comput Environ Urban Syst 35:358–367. https://doi.org/10.1016/j.compenvurbsys.2011.02.001
Ichinose T, Shimodozono K, Hanaki K (1999) Impact of anthropogenic heat on urban climate in Tokyo. Atmos Environ 33:3897–3909. https://doi.org/10.1016/s1352-2310(99)00132-6
Japan District Heating & Cooling Association (2013) "Chiiki reidambo gijutsu tebikisho kaiteidai4han" . Japan District Heating & Cooling Association, Tokyo, p 31
Japanese Standards Association (2008) JIS B 8609: Performance tests of mechanical draft cooling tower. Japanese Industrial Standard/Japanese Standards Association.
Jin K, Wang F, Chen D, Liu H, Ding W, Shi S (2019) A new global gridded anthropogenic heat flux dataset with high spatial resolution and long-term time series. Sci Data 6:139. https://doi.org/10.1038/s41597-019-0143-1
Kimura F, Takahashi S (1991) The effects of land-use and anthropogenic heating on the surface temperature in the Tokyo Metropolitan area: A numerical experiment. Atmos Environ Part B Urban Atmos 25:155–164. https://doi.org/10.1016/0957-1272(91)90050-o
Li X, Zhou Y, Yu S, Jia G, Li H, Li W (2019) Urban heat island impacts on building energy consumption: A review of approaches and findings. Energy 174:407–419. https://doi.org/10.1016/j.energy.2019.02.183
Lin LZ, Su F, Fang QL, Ho HC, Zhou Y, Ma H, Chen D, Hu L, Chen G, Yu H, Yang B, Zeng X, Xiang M, Feng W, Dong G (2022) The association between anthropogenic heat and adult hypertension in Northeast China. Sci Total Environ 815:152926. https://doi.org/10.1016/j.scitotenv.2022.152926
Madaniyazi L, Zhou Y, Li S, Williams G, Jaakkola JJK, Liang X, Liu Y, Wu S, Guo Y (2016) Outdoor Temperature, Heart Rate and Blood Pressure in Chinese Adults: Effect Modification by Individual Characteristics. Sci Rep 6:21003. https://doi.org/10.1038/srep21003
Ministry of Land, Infrastructure, Transport and Tourism, Ministry of the Environment (2004) "Heisei 15nendo toshi ni okeru jinkohainetsu yokusei ni yoru hitoairando taisaku chosahokokusho." https://www.env.go.jp/air/report/h16-05/. Accessed 15 Dec 2022
Ministry of the Environment (2022) "netchushokankyohokemmanyuaru 2022". https://www.wbgt.env.go.jp/heatillness_manual.php. Accessed 15 Dec 2022
National institute for land and infrastructure management (2014) CFD on Excel. http://www.nilim.go.jp/lab/icg/hyoukatool.htm. Accessed 06 Dec 2022
Navarro L, de Gracia A, Niall D, Castell A, Browne M, McCormack SJ, Griffiths P, Cabeza LF (2016) Thermal energy storage in building integrated thermal systems: A review. Part 2. Integration as Passive System, Renew Energy 85:1334–1356. https://doi.org/10.1016/j.renene.2015.06.064
Sailor DJ (2011) A review of methods for estimating anthropogenic heat and moisture emissions in the urban environment. Int J Climatol 31:189–199. https://doi.org/10.1002/joc.2106
Ueno T, Takahashi K, Sumiyoshi D (2019) Estimation for energy demand fluctuation in commercial and business area by monte carlo simulation. J Environ Eng 84:291–301. https://doi.org/10.3130/aije.84.291
United Nations (2022) World population prospects (2022). Department of Economic and Social Affairs, UN Population Division. https://www.un.org/development/desa/pd/sites/www.un.org.development.desa.pd/files/wpp2022_summary_of_results.pdf. Accessed 15 Dec 2022
Yanai T, Murakami S, Ishino H, Shinagawa K, Fujii T, Abe H, Ito S (2011) Development of an integrated energy simulation tool for buildings and MEP systems, the BEST (Part 88): Outline of equipment characteristics and theme in the future. Technical Papers of Annual Meeting the Society of Heating, Air-conditioning and Sanitary Engineers of Japan 2011.2: 1715–1718. https://doi.org/10.18948/shasetaikai.2011.2.0_1715
Yang L, Yan H, Lam JC (2014) Thermal comfort and building energy consumption implications – a review. Appl Energy 115:164–173. https://doi.org/10.1016/j.apenergy.2013.10.062
Yuan C, Zhu R, Tong S, Mei S, Zhu W (2022) Impact of anthropogenic heat from air-conditioning on air temperature of naturally ventilated apartments at high-density tropical cities. Energ Build 268: 112171. https://doi.org/10.1016/j.enbuild.2022.112171

Publisher's Note